

Supplemental Information for:

Structural Basis for the Trembler-J Phenotype of Charcot-Marie-Tooth Disease

Masayoshi Sakakura, Arina Hadziselimovic, Zhen Wang,

Kevin L. Schey, and Charles R. Sanders*

Department of Biochemistry and Center for Structural Biology, Vanderbilt University School of Medicine,

Nashville, Tennessee 37232-8725 USA

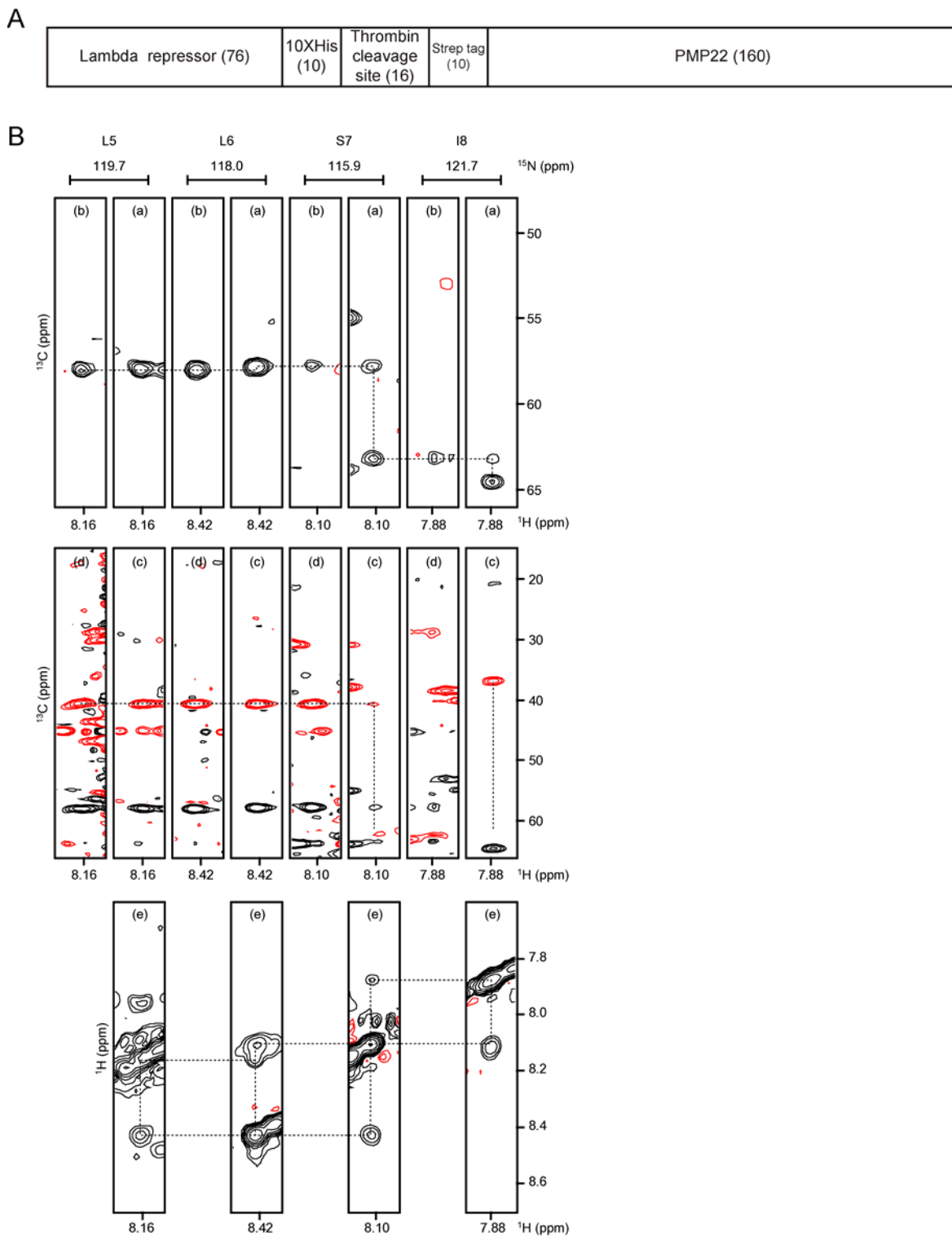


Figure S1, related to Figure 1. Fusion protein construct used for expression PMP22 and examples of NMR data used for backbone resonance assignments of PMP22. (A) Diagram of fusion protein used for protein expression. The numbers in parentheses indicate the length of each segment. The lambda repressor domain represents residues 1-76 of the E. coli lambda repressor, the thrombin cleavage site has a sequence of LVPRGS, and the strep tag has a sequence of WSHPQFEK. (B) Sections of ^{13}C - ^1H slices from TROSY-based

(a) HNCA, (b) HN(CO)CA, (c) HNCACB, (d) HN(CO)CACB spectra, and (e) ^1H - ^1H slices from a ^{15}N -separated NOESY-TROSY spectrum of uniformly- ^2H , ^{13}C , ^{15}N -labeled PMP22 in TDPC micelles at 45 °C and 800MHz. Slices from 3-D spectrum corresponding to the protein segment Leu5-Ile8 are indicated. Sequential C_α and C_β connections are indicated by dotted horizontal lines. Note that unambiguous sequential connection is not achieved in ^{13}C -based spectra because of the chemical shift degeneracy (Leu5-Leu6) and an overlap of $^{13}\text{C}_\alpha$ and $^{13}\text{C}_\beta$ signals (Ser7). The characteristic $^1\text{H}_\text{N}$ - $^1\text{H}_\text{N}$ NOE pattern associated with helices facilitated unambiguous assignments for the residues with poor triple resonance information.

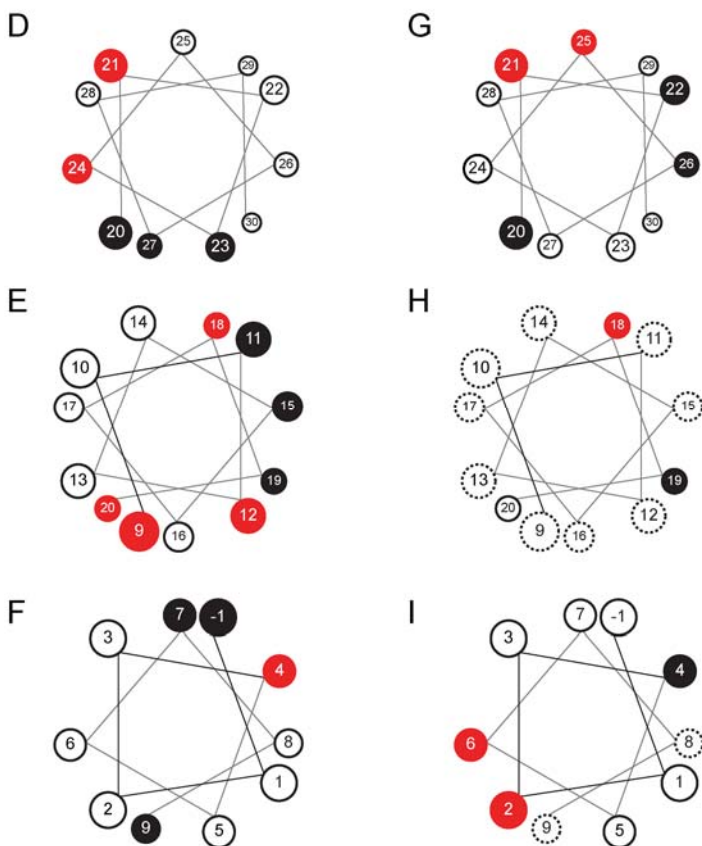
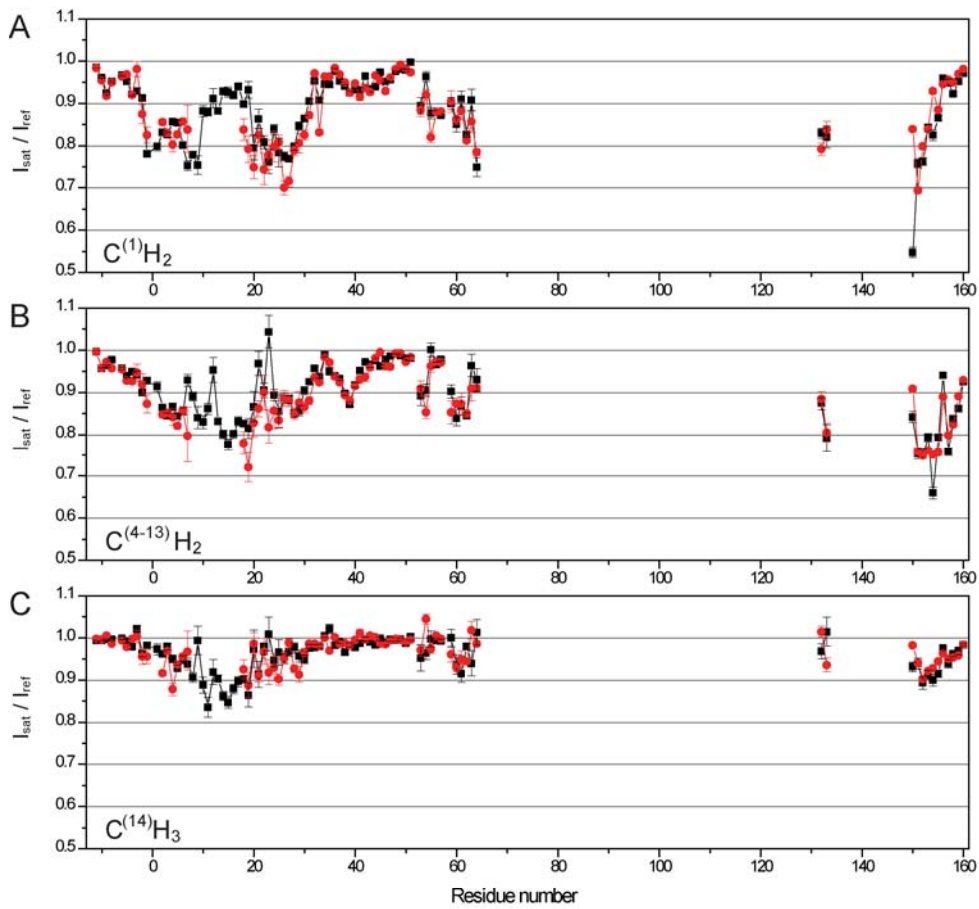


Figure S2, related to Figure 4. STD-NMR results for interaction of WT and PMP22 with its host detergent, TDPC.

Panels A-C show the site-specific degree of backbone amide TROSY peak saturation for WT (black symbols) and TrJ (red symbols) when either the C⁽¹⁾ methylene nearest the head group of TDPC was saturated (panel A), the entire region of the tetradecyl chain (panel B), or the terminal methyl group of the tetradecyl chain (panel C). Panels D-I summarize the STD measurements for sites that are mapped onto helical wheel diagrams. Panels D-F represent WT PMP22, while panels G-I represent TrJ. Panels D, F, G, and I indicated STD involving presaturation of the methylene closest to the headgroup on TDPC's tetradecyl chain. Panels E and H reflect results from when the terminal methyl group at the end of the tetradecyl chain is irradiated. Black sites indicate the face most strongly impacted by saturation from the irradiated detergent groups while red sites indicate the sites least impacted by saturation transfer.

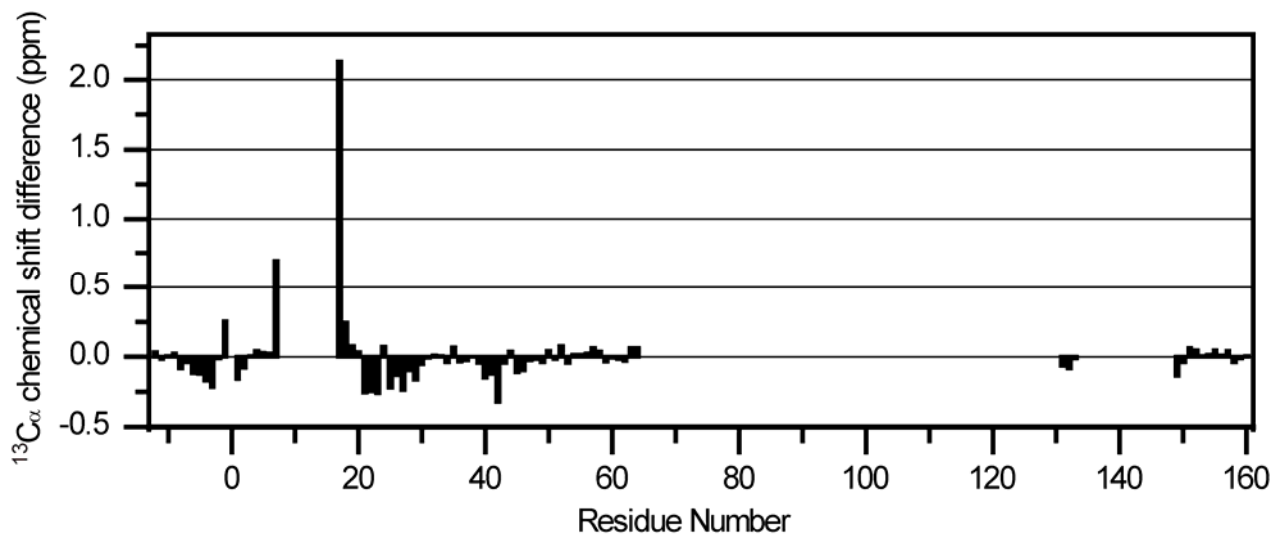


Figure S3, related to Figure 1E. Differences in $^{13}\text{C}_\alpha$ NMR chemical shifts between wild type and TrJ PMP22 in TDPC micelles at 45°C.

Table S1, related to Figure 2: Summary of correlation time and diffusion coefficient measurements and calculated sizes.

	τ_c (ns)	D_t ($\text{m}^2 \text{sec}^{-1}$)	$R_{h,t}$ (\AA)	MW
PMP22	16 ± 2	$7.7 (\pm 0.1) \times 10^{-11}$	33	58 K
TDPC micelle (276 mM TDPC)		$8.6 (\pm 0.1) \times 10^{-11}$ *	28	47 K

τ_c : correlation time derived from ^{15}N T_1 and T_2 measurements

D_t : translational diffusion coefficient

$R_{h,t}$: hydrodynamic radius of the micelle or protein-detergent mixed micelle based on measured D_t and assuming spherical shape

MW : aggregate molecular weight of micelle or protein-detergent mixed micelle based on measured D_t and assuming spherical shape

* D_t value of $9.06 \times 10^{-11} \text{ m}^2 \text{sec}^{-1}$ was used to back-calculate the viscosity.